Theses market - possible topics introduction (from 2025)

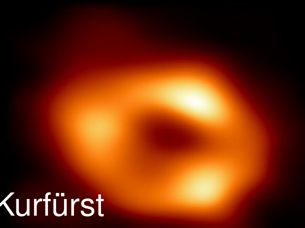

Petr Kurfürst
Masaryk University (MU), Brno, Czech Republic

ÚTFA seminary - October 4, 2024

Interacting supernovae - red supergiant with $M = 15\,M_\odot$ and $R = 1000\,R_\odot$ (Kurfürst+ 2020)

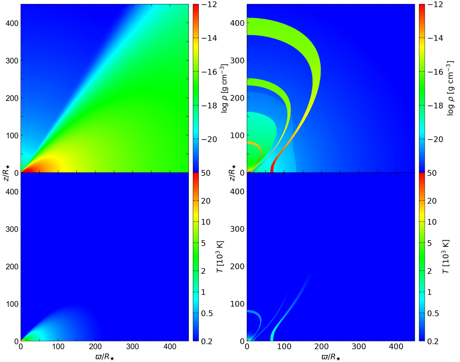

- Illustrations of the initial states: **Left** - SN-disk interaction, **right** - SN-lobes interaction

Ambient medium:

The initial ρ profiles in SN-disk model -

$$\rho_{\rm disk} = \rho_{0,\rm disk} \left(\frac{R_\star}{r}\right)^w \exp\left[\frac{2\,(\sin\theta - 1)}{(H/\mathcal{R})^2}\right],$$

where $\rho_{0,\rm disk} \approx 5 \times 10^{-14}\,\rm g\,cm^{-3}$ is the mass density at the base of the disk midplane, $w = 2$ is the power-law index, $H = c_S/\Omega$ is the disk vertical scaleheight, and $\mathcal{R}$ is the radial distance measured in the disk equatorial plane.

We set the bipolar lobes similar to the Homunculus nebula with reduced size so the total mass of the nebula is thus $\approx 1.7 \times 10^{-2}\,M_\odot$.

SN-CSM interactions for two CSM types - disk and bipolar lobes

- Progenitor star - RSG with $M = 15\,M_\odot$ and $R = 1000\,R_\odot$
- **Evolution of hydrodynamic profiles** at $t \approx 700$ d (simulation time)

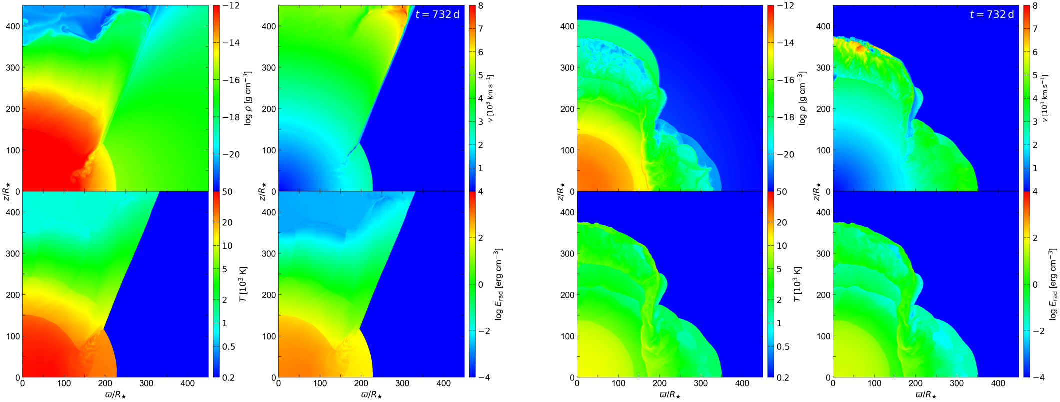

- **Left:** SN-disk interaction, ρ, v, T, and $E_{\rm rad}$, **Right:** same for SN-lobes interaction

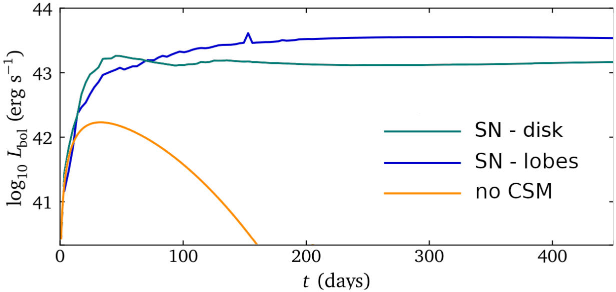

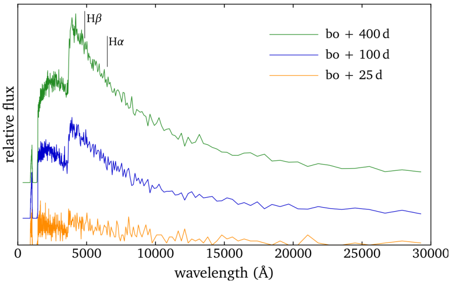

Calculation of light curves (left) **and introductory spectra model** (right) using the 3D MC-RT code. For comparison, we plotted the light curve without an interaction with CSM.

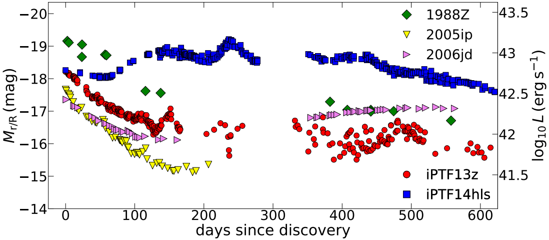

Observed light curves of several prominent long-lasting SLSNe.

Galactic center - inner ∼1 pc is a region of mutual interactions of stars, gas, and dust within the gravitational potential of the SMBH (Zajaček+ 2020)

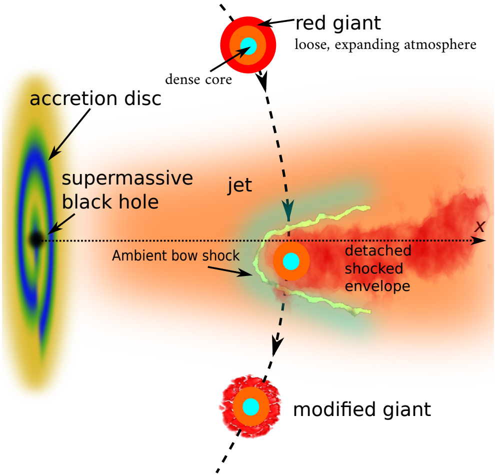

- Illustration of the jet - RG interaction

Ambient medium:

The ρ and T profiles of the ambient plasma -

$$n_{\rm a} \approx n_{\rm B} \left(\frac{r}{r_{\rm B}}\right)^{-1}, \quad T_{\rm a} \approx T_{\rm B} \left(\frac{r}{r_{\rm B}}\right)^{-1},$$

$n_{\rm B} = 26\,{\rm cm}^{-3}$, and $T_{\rm B} = 1.5 \times 10^7\,{\rm K}$ are the number density and the T at the Bondi radius.

The **number density** can be estimated as

$$n_{\rm j} = \frac{L_{\rm j}}{\mu m_{\rm H} (\Gamma - 1) c^2 v_{\rm j} \pi x^2 \tan^2 \theta}$$

and $M_\bullet = 4 \times 10^6\, M_\odot$

Example: **Star-jet interactions at the orbital distance** 10^{-3} **pc,** $L_j = 10^{42}$ **erg s**$^{-1}$

- Jet luminosity $L_j = 10^{42}\,\mathrm{erg\,s^{-1}}$, jet velocity $v_j = 0.66\,c$
- **Star crosses the jet** for the first time at $t \approx 15$ d (simulation time)

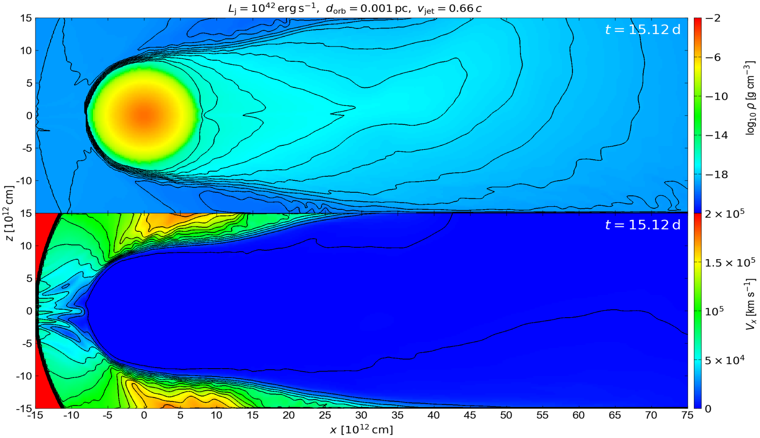

Example: **Star-jet interactions at the orbital distance 10^{-3} pc, $L_j = 10^{42}\,\mathrm{erg\,s^{-1}}$**

- Jet luminosity $L_j = 10^{42}\,\mathrm{erg\,s^{-1}}$, jet velocities $v_j = 0.33\,c$, $0.66\,c$
- **Graph of the relative mass ablated**, up to 10 passages

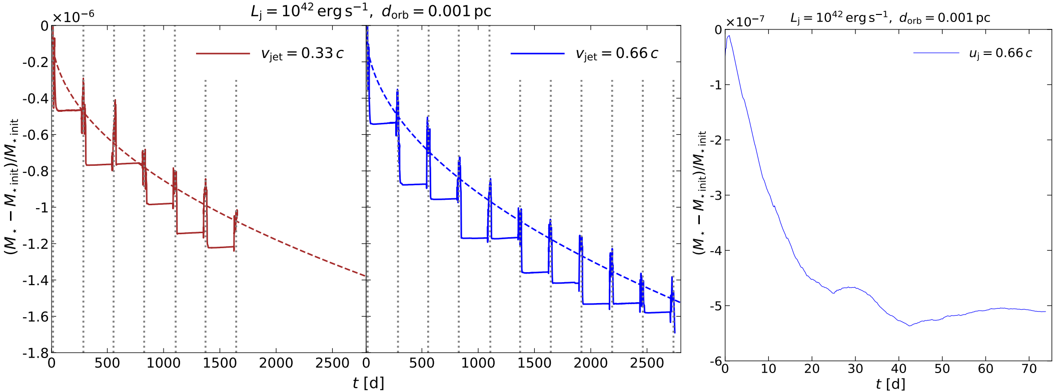

- Power-laws $\Delta M_1(t)\,[M_\odot]$: $-3.36 \times 10^{-8}(t/1\,\mathrm{day})^{0.47}$ (L) $-3.12 \times 10^{-8}(t/1\,\mathrm{day})^{0.49}$ (R)
- Σ mass loss $\Delta M_1\,[M_\odot]$ (AGN): -1.16×10^{-4} (L), -1.58×10^{-4} (R): $\approx$ analytical ΔM_1^{max}.

• Magnetospheres of hot stars

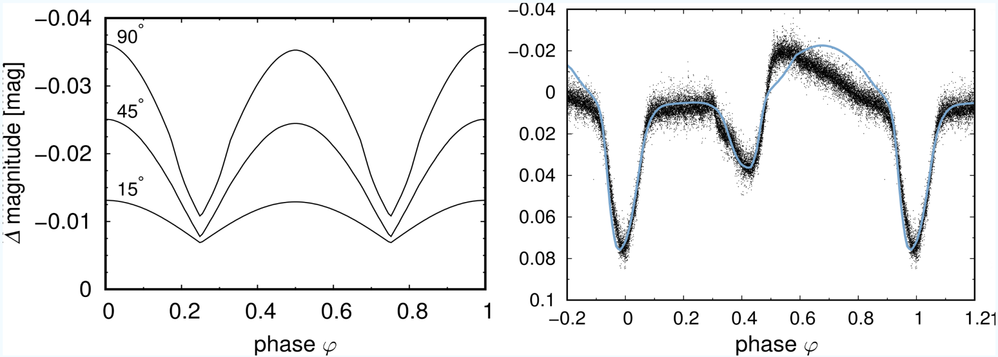

Figure 1. **Semianalytical calculations of a light curve.** Left: Light curves from circumstellar magnetosphere emission - a dipolar magnetic field with $\psi = 90°$ and different inclinations. Right: Simulated light curve assuming a combined dipole and quadrupole magnetic field and accounting for absorption and emission in the magnetosphere. Compared with the observed light curve of the star σ Ori E. From Krtička et al. (2022).

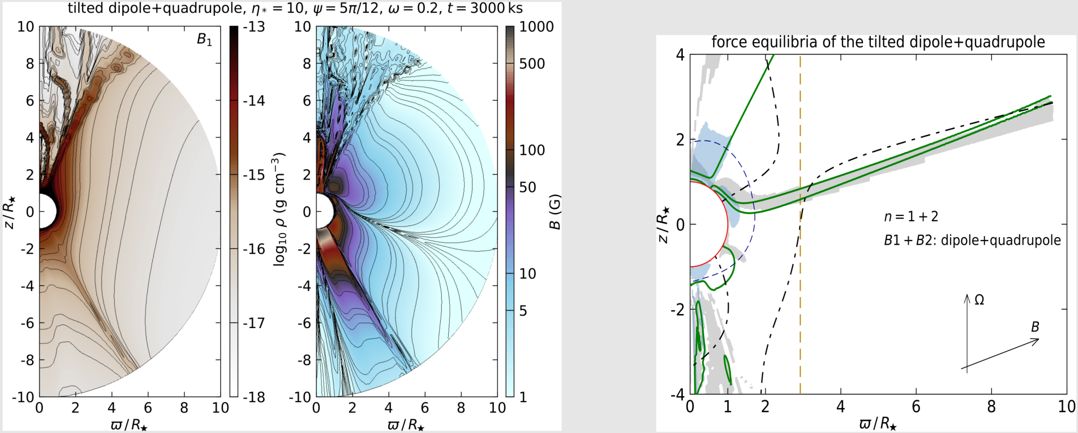

Figure 3. **Tilted dipole + quadrupole magnetosphere.** 2D radial-vertical slices of the density (left), magnitude of the magnetic field (centre), and equilibrium surfaces configuration (right).

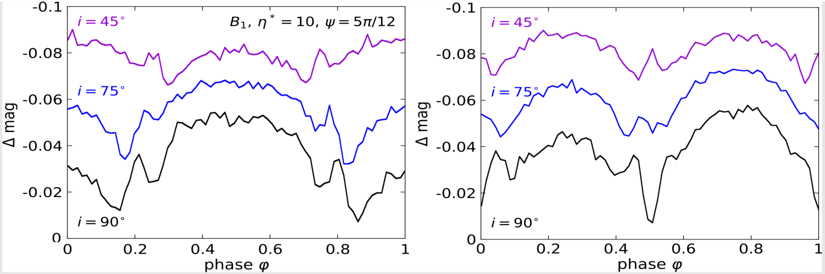

Figure 4. **Numerical calculations of light curves.** Top: tilted dipole, bottom: tilted dipole + quadrupole.

Section "Model set-up". The left panel of Fig. 4 shows light curves of the tilted dipole, taking into account the absorption and emission. The minima and maxima are roughly at the same phase as in the analytical model shown in the left panel of Fig. 1; however, due the inclusion of the absorption (unlike the analytical solution where only the emission is calculated), we obtain different minima and maxima amplitudes for different observers' inclinations. The right panel of Fig. 4 shows the light curves of the tilted dipole + quadrupole combination, representing an approximate numerical counterpart of the analyti model given in the right panel of Fig. 1. The basic similarity in phase and amplitude asymmetry is obvious; deviations in details can be explained by the different angle ψ.